Supplementary Material

Thermal profiles associated with nest site selection of Nile crocodiles (*Crocodylus niloticus*) on a commercial crocodile farm

Appendix A: Supplementary figures

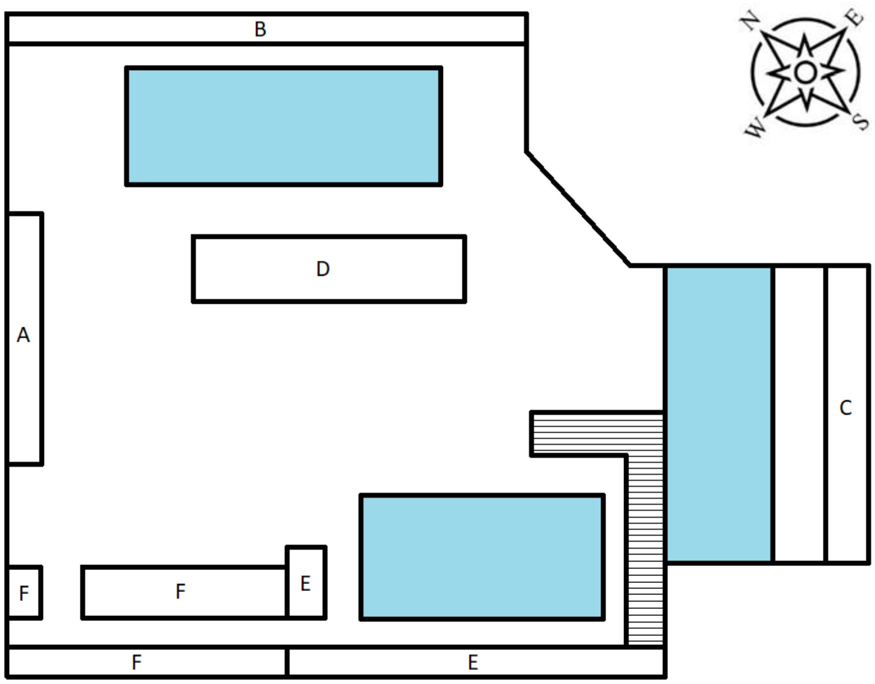

Figure A1. A not-to-scale diagram of the study site, showing the placements of nesting sections A–F. The walkway is represented with horizontal-lines, and the waterbodies are colored blue.

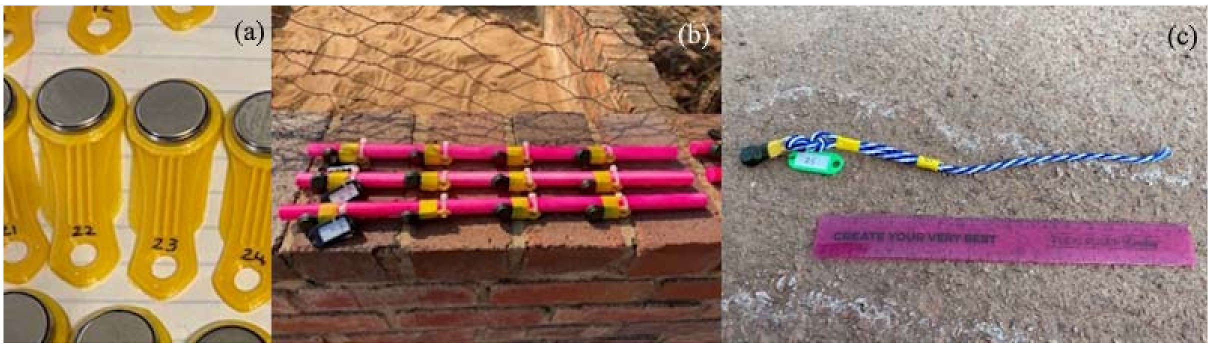

Figure A2. Images of (a) the 3D printer holders, (b) dowel iButtons, and (c) single iButtons.

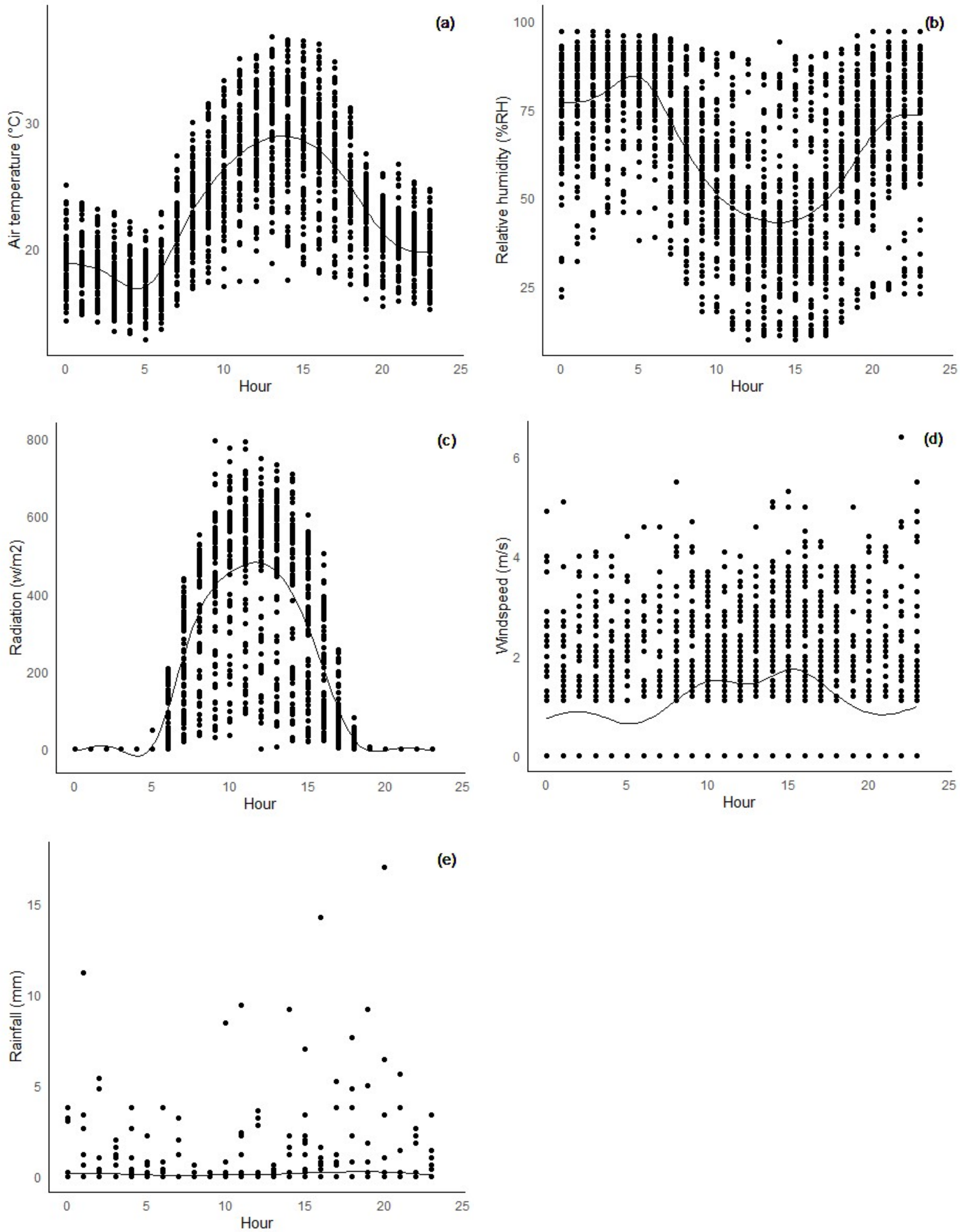

Figure A3. Hourly (a) air temperature (°C), (b) relative humidity (% RH), (c) solar radiation (W/m^2), (d) wind speed (m/s), and (e) rainfall (mm) throughout the nesting period (October–December 2022). Solid lines represent the mean per hour.

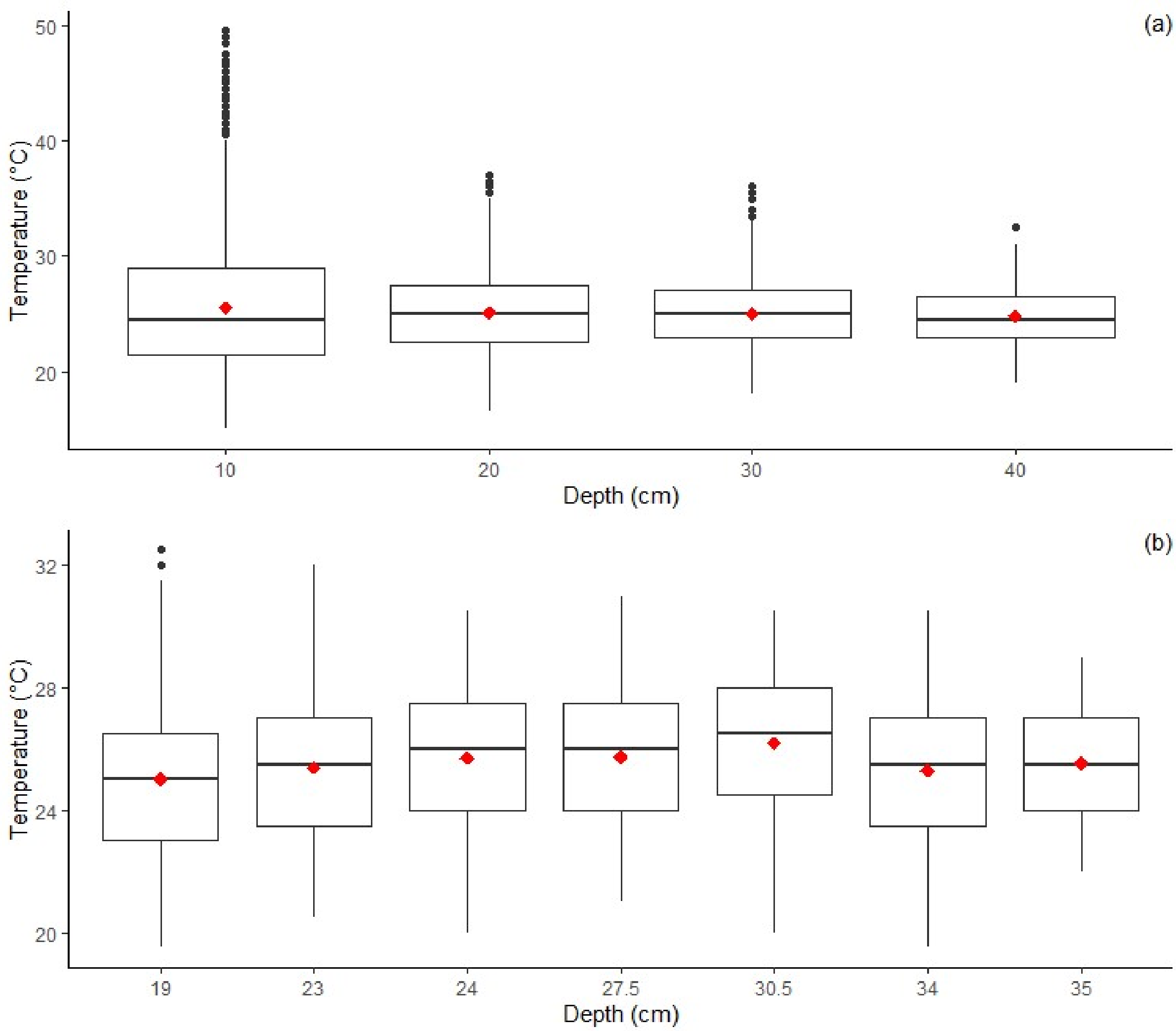

Figure A4. Sand temperatures recorded at varying depths below ground level. Plot (a) depicts measurements from dowel iButtons placed at 10, 20, 30, and 40 cm below the surface, and (b) depicts temperatures from harvested nest sites, specifically at the depth of the deepest egg, using single iButtons. Each boxplot displays the median (centre line), interquartile range (box edges), and 1.5 * IQR (whiskers). Points beyond the whiskers represent outliers and means are represented by red rhombuses.

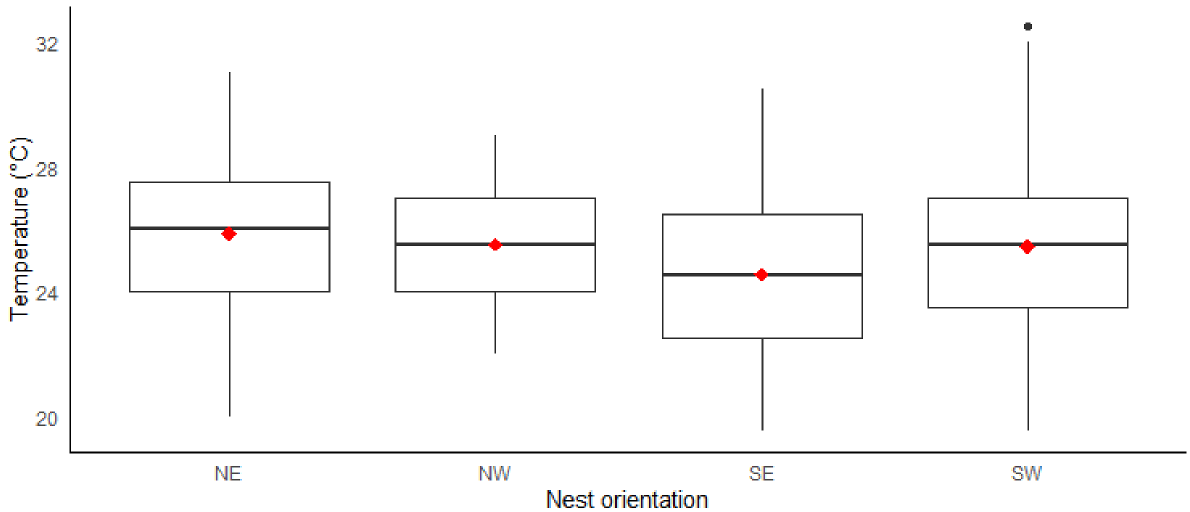

Figure A5. Single iButton sand temperatures recorded in each nest orientation. Each boxplot displays the median (centre line), interquartile range (box edges), and 1.5 * IQR (whiskers). Points beyond the whiskers represent outliers and means are represented by red rhombuses.

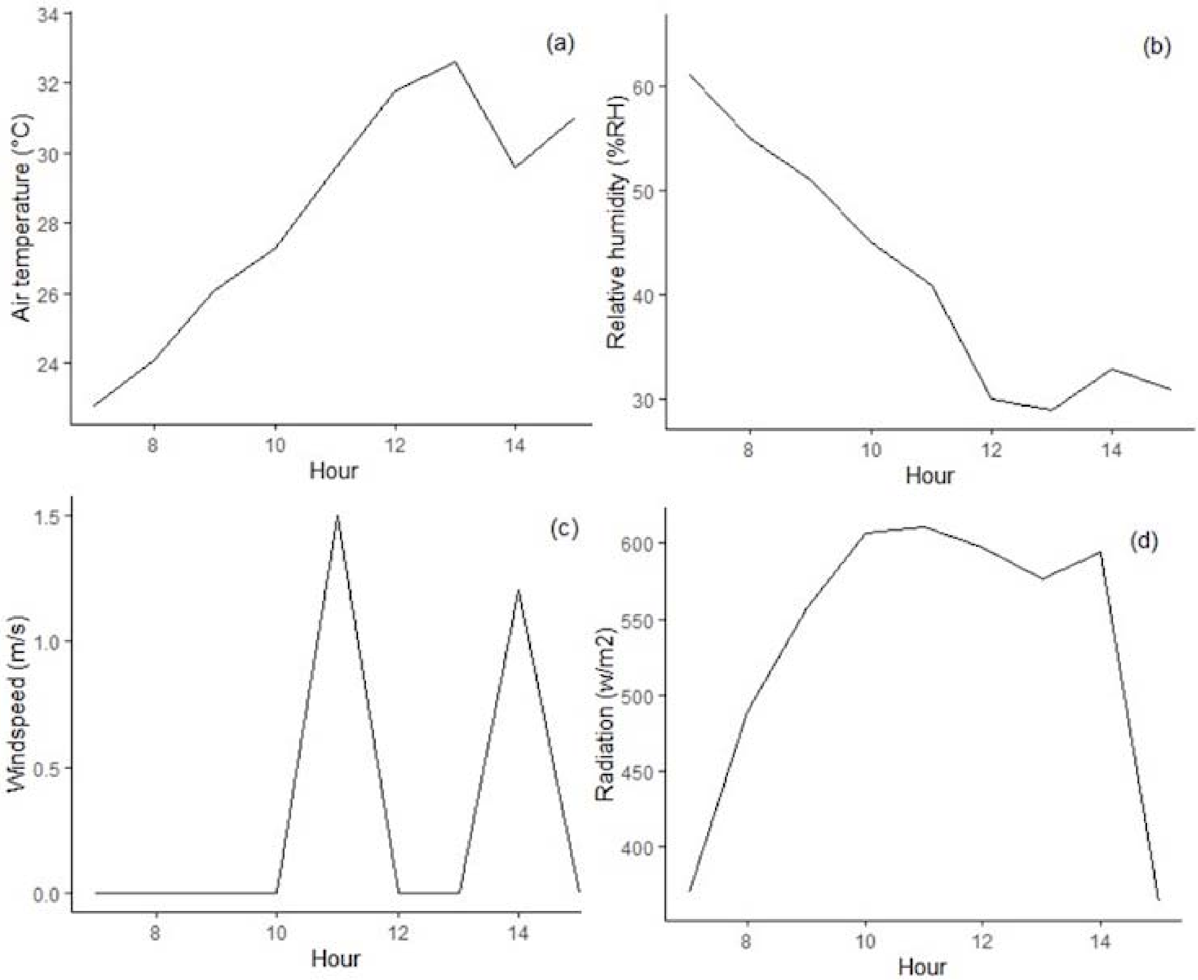

Figure A6. Depicts the hourly (a) air temperature (°C), (b) relative humidity (% RH), (c) wind speed (m/s), and (d) radiation (W/m^2) on 1 December 2022.

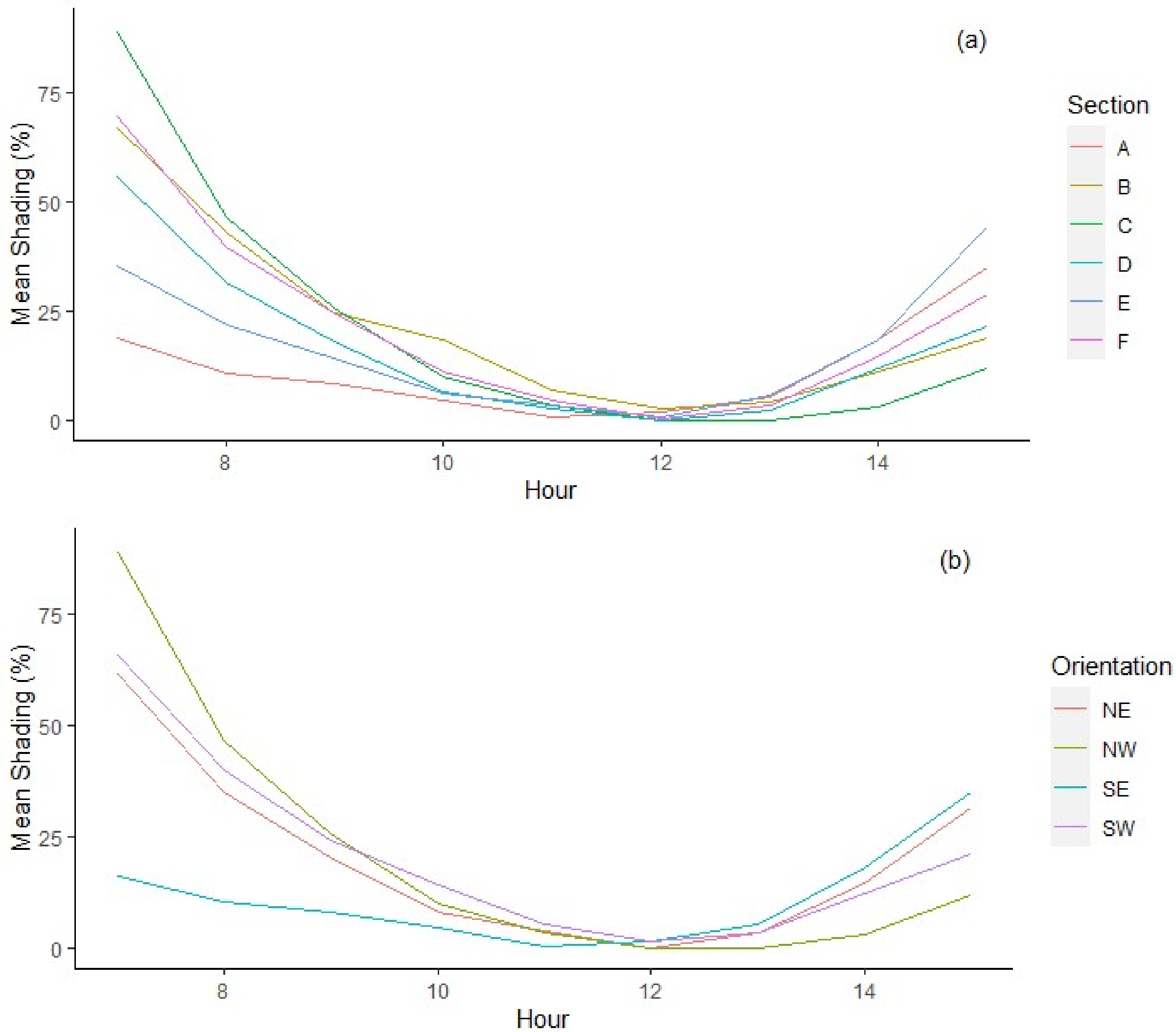

Figure A7. Mean hourly shading percentage over nesting sites per (a) nesting section and (b) nesting orientation.

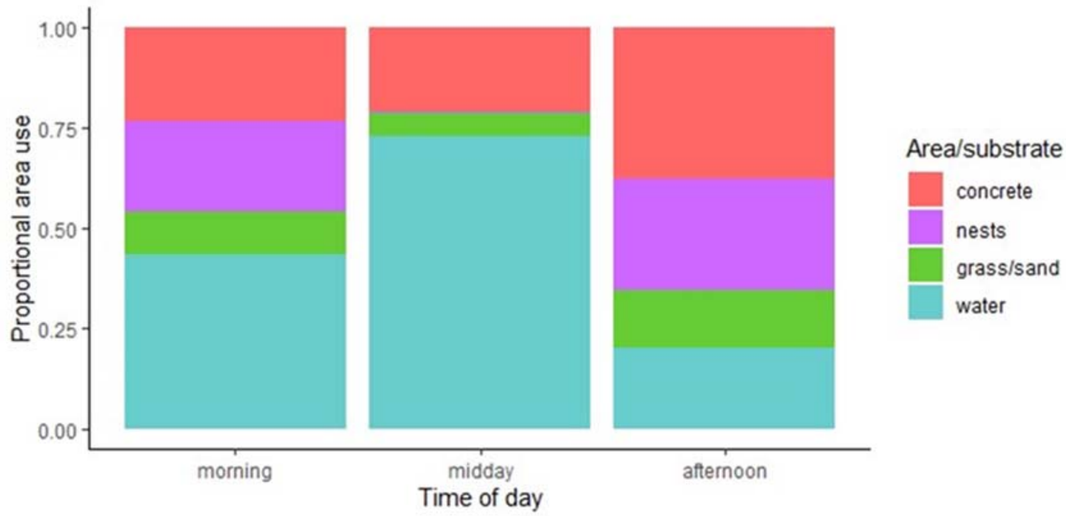

Figure A8. Proportional pen area/substrate use per time of the day, categorized into morning (before 11:00), midday (12:00–13:00), and afternoon (after 15:00).

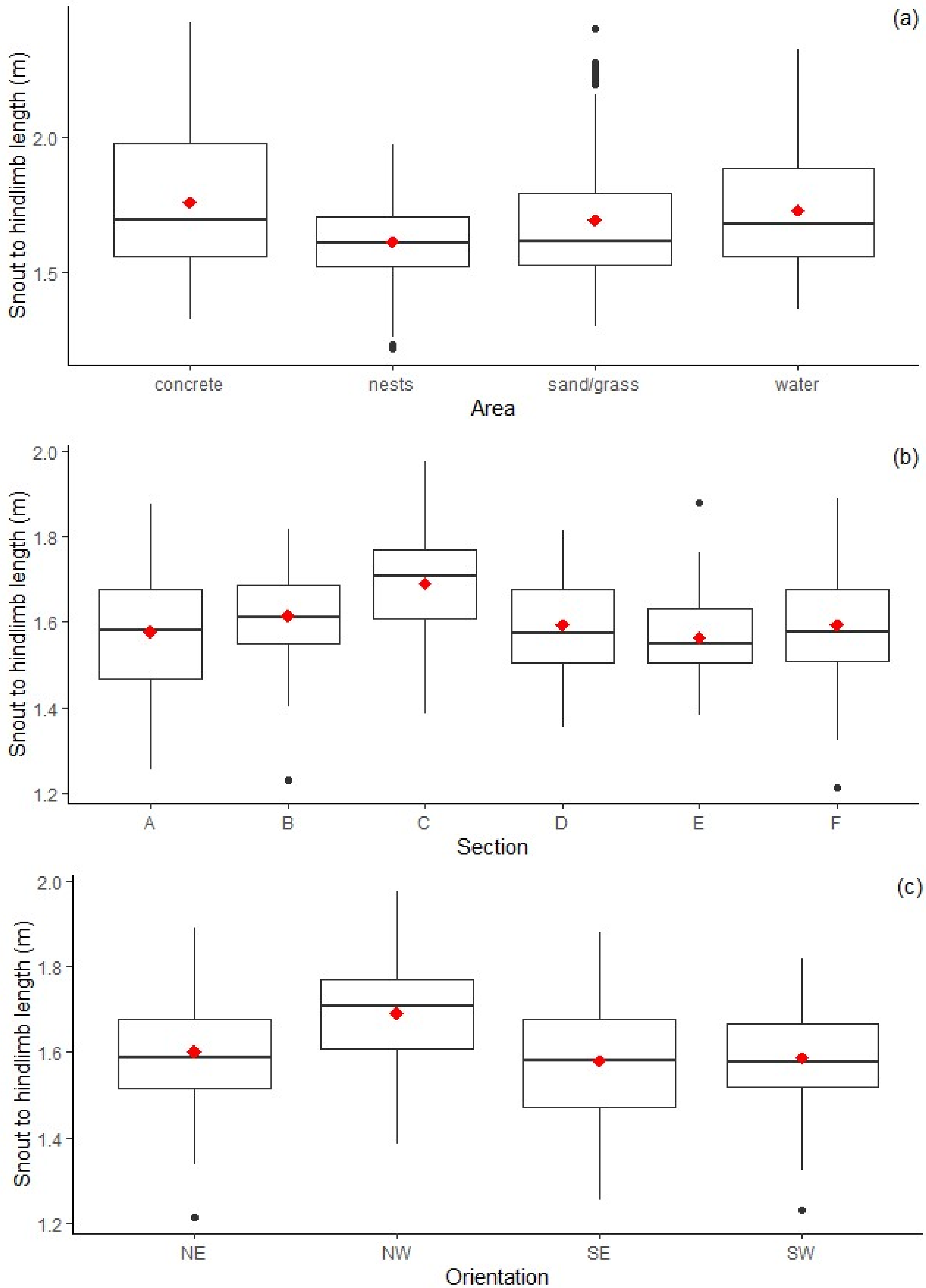

Figure A9. SHL of the crocodiles occupying the various pen areas (a), nesting sections (b), and nesting orientations (c). Each boxplot displays the median (centre line), interquartile range (box edges), and 1.5 * IQR (whiskers). Points beyond the whiskers represent outliers and means are represented by red rhombuses.

Appendix B: Nest depth evaluation on a commercial crocodile farm

Nest depths were evaluated early in the nesting season to identify the most appropriate depths for the assessment of the thermal profiles within nests in the pen that was eventually selected. Various depths within 32 nests, across three pens, were measured upon egg extraction. Egg extractions occurred daily in the early hours of the morning (05:00–07:00), when the crocodiles were least active, throughout the nesting season. A team of three experienced farm personnel identified nesting sites where digging/nesting by a crocodile had occurred. The procedures for egg collection were conducted in accordance with Section 7 of the South African National Standard for Crocodiles in Captivity (SANS, 2009). Following egg collections, the nests were raked flat, ensuring any new nest digging activity would be spotted the following day. Breeder pens on the farm were built between 1990–1996 and although river sand was used to fill all nesting sites, sand consistency variations were noticed during excavations. Of the 32 nests, 16 were from nests with coarse and loosely packed sand, and 16 were from nests with densely packed fine sand. The first measure was the depth of the last egg deposited (most shallow) by the nesting female, from the top of the egg to ground surface level. The second measure was the depth at which the first egg was deposited (deepest) by the nesting female, measured from the top of the egg to the ground surface level. These two measures were then used to determine the overall nest depth of the full nest (the difference between the deepest and shallowest egg depths). Two of the 32 nests had a single egg sitting at or just below ground level, > 10 cm from the rest of the nest's eggs, these eggs were omitted.

Shallowest egg depths ranged from 10.00–18.00 cm ($\bar{x}$ = 13.47 cm, SD = 2.29 cm, SE = 0.57 cm) for nests with coarse sand, and from 10.5–24.5 cm ($\bar{x}$ = 17.03 cm, SD = 4.18 cm, SE = 1.04 cm) for nests with fine sand. Deepest egg depths ranged from 27.00–33.50 cm ($\bar{x}$ = 29.72 cm, SD = 1.84 cm, SE = 0.46 cm) for coarse sanded nests, and from 18.00–39.00 cm ($\bar{x}$ = 29.06 cm, SD = 5.16 cm, SE = 1.29 cm) for fine sanded nests. Nest depths ranged from 11.00–20.50 cm ($\bar{x}$ = 16.25 cm, SD = 2.74 cm, SE = 0.69 cm) for coarse sanded nests, and from 3.00–17.00 cm ($\bar{x}$ = 12.03 cm, SD = 3.56 cm, SE = 0.89 cm) for fine sanded nests. Four out of 32 nests had nest depths < 10 cm where the eggs were spread over a larger diameter than in other measured nests. The shallowest egg depth and total nest depths measured varied significantly ($P < 0.05$, $t = -2.991$, $df = 23.276$; $P < 0.001$, $t = 3.753$, $df = 28.172$, respectively) between the different sand types. The fine sanded nests had more compact nest depths, with the first eggs buried deeper than those of the coarse sanded nests. The deepest egg depths did not vary significantly between sand types (figure A9).

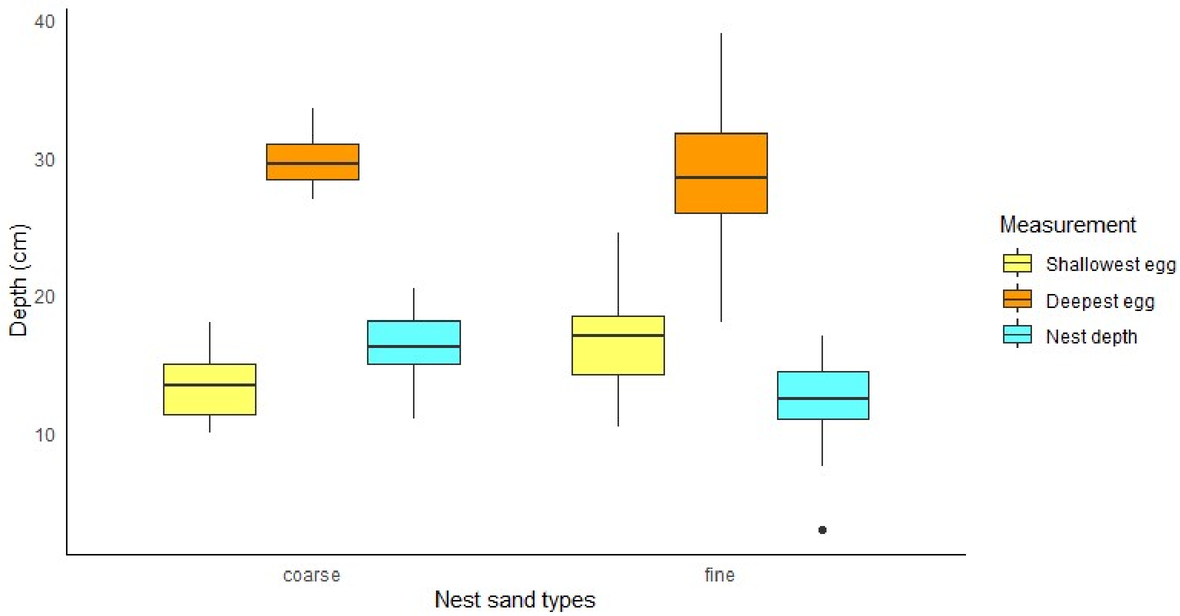

Figure B1. Nest depth variables (shallowest egg, deepest egg, and nest depth) between coarse and fine sanded nests on a commercial Nile crocodile farm in South Africa. Each boxplot displays the median (centre line), interquartile range (box edges), and 1.5 * IQR (whiskers). Points beyond the whiskers represent outliers.

Farmed crocodile nest depths in the present study were consistent with previous wild Nile crocodile nest studies (Pooley & Gans, 1976; Kofron, 1989; Hartley, 1990; Swanepoel *et al.*, 2000). Farmed Nile crocodile nest construction varied between nest sand types (coarse versus fine) with regards to shallowest egg depths and overall nest depths. This could have been due to varying ease of nest construction depending on the sand types. Nests with densely packed fine sands resulted in shallower total nest depths, with the first eggs laid at deeper depths than in coarse sanded nests. The loose consistency of coarse-sanded nests likely impacted the stability/uniformity of the nests dug into that sand type. If the sand constantly fell back inward during digging, the result would be a narrower nesting space, potentially explaining why the deepest eggs were comparably deep with fine sanded nests but the final eggs laid were shallower, increasing overall nest depths. Not all assessed nests were spherical, some were tightly packed, whilst others were spread out in a flatter topography. This suggests different nesting strategies were employed by the nesting females, based on sand type. These findings concur with Kofron (1989), where soil type affected Nile crocodile nest cavity structure/shape as follows: bowl-shaped nests were produced in loose sand nests, funnel-shaped nests in loose sands with firm substrate, and “roofed” downward slanting nests in firm soils. Soil particle size has also been implicated in the thermal regimes of crocodile nests (Somaweera & Shine, 2013). In the current study, the deepest egg depths recorded between nests with the two sand-types did not differ. This could be attributed to the comparable size of the breeding females (similar digging capabilities) or to instinctual behaviour, such as a preferred 'default' depth for nesting. The preferred depth for the deepest egg, whether chosen for nest stability, optimal incubation conditions, protective measures against predators or adverse weather, or some unknown factor(s) remained consistent regardless of the sand type.

Appendix C: Supplementary tables

Table C1. Nest site divisions by section, orientation, number of nests per section, mean distance from the closest water body, and mean distance from the tourist walkway.

Nest section	Orientations	Number of nesting sites	Mean distance from water (m)	Mean distance from walkway (m)
A	SE	17	22.3	47.9
B	SW	22	4.5	45.2
C	NW	11	7.3	16.8
D	NE & SW	14 & 14	14.3	19.6
E	NE & SE	11 & 4	4.3	23.2
F	NE, SE & SW	21, 3 & 9	20.4	46.1

Table C2. Descriptive statistics for the temperatures (°C) recorded by iButtons deployed on dowels, ordered by section and depth (cm).

iButtons	Section	Depth	Min	Max	Mean	SE
1, 5, 9	A	10	15.5	49. 5	24.9	0.06
2, 6, 10		20	16.5	35.5	24.4	0.04
3, 7, 11		30	18	35	24.4	0.03
4, 8, 12		40	19	32.5	24.2	0.03
13, 17, 21	F	10	15	46.5	26.1	0.07
14, 18, 22		20	17.5	37	25.8	0.05
15, 19		30	19.5	36	25.9	0.04
16, 20, 24		40	20	30.5	25.4	0.03

Table C3. Descriptive statistics for the temperatures (°C) recorded by iButtons deployed as singles, ordered by depth (cm).

iButtons	Section	Orientation	Depth	Min	Max	Mean	SE
32	B	SW	19	19.5	32.5	25.0	0.05
27	C	NW	19.5	22	38	28.7	0.06
34	D	SW	23	20.5	32	25.4	0.06
38	F	NE	24	20	30.5	25.7	0.05
30	F	NE	27.5	21	31	25.7	0.05
28	D	NE	30.5	20	30.5	26.2	0.05
31	A	SE	34	19.5	30.5	24.6	0.06
44	F	SW	34	21	30.5	25.9	0.04
33	C	NW	35	22	29	25.5	0.04

*The only nesting section not represented by a single iButton was section E. A single iButton in section C, buried at a depth of 19.5 cm below ground level, malfunctioned and the outputs of that logger are not included in the analyses that follow.

Table C4. Descriptive statistics of drone-derived crocodile back temperatures, positional temperatures, surface temperatures of crocodile-occupied nests, crocodile SHLs, and climate variables on the day of the thermal flights (1 December 2022).

Variable	Min	Max	Mean	SE
Crocodile back temperatures (°C)	17.4	50.6	30.6	0.1
Crocodile positional temperatures (°C)	15.1	56.3	29	0.2
Nest surface temperatures (°C)	19.3	31.1	23.6	0.2
Snout-hindlimb lengths (m)	1.2	2.3	1.6	0.0
Air temperature (°C)	22.8	32.6	28.1	0.0
Relative humidity (% RH)	29	61	42	0.3
Wind speed (m/s)	0	1.5	0.3	0.0
Solar radiation (W/m^2)	364.1	610.9	523.7	2.3

Table C5. Nest surface temperature (°C) descriptive statistics per nesting section between 07:00 and 15:00, on 1 December 2022.

Section	Min	Max	Mean	SE
A	23.1	50.0	36.8	0.5
B	20.3	66.4	36.9	0.8
C	19.3	53.7	36.6	1.0
D	20.8	67.3	42.6	0.8
E	20.2	50.0	34.8	0.5
F	20.8	66.7	46.8	0.7